Tail Team: Final Report

24-775: Robot Design and Experimentation

Date: 05/03/22

Team: Ryan Tarr, Zach Nobles, Harshal Vakhariya, Pranav Katragadda, Saurabh Patil, Aishwarya Ravi

Abstract

Animals use tails for a variety of different actions, especially to maintain balance. Recent research has worked off of this bio-inspiration [1] and established tails as a great mechanism to balance robots during locomotion and turning. The purpose of this project is to compare the maneuverability during turns of a wheeled robot with an aerodynamic tail to one with an inertial (rigid) tail. It is our hypothesis that the aerodynamic tail will outperform its inertial counterpart in this regard. The inertial tail analysis is based on the work of Patel *et al*. [1] which looked at the turning speed and lateral acceleration of a wheeled RC car using a tail with an attached mass at the end of the rod. These results were compared to the same metrics measured without a tail attached to the system. Team Tail is looking to expand on this work by procuring our own results based on Patel's work and comparing them to the results obtained from an aerodynamic tail that utilizes drag force to mimic the resistance produced by the mass at the end of the inertial tail. Our hypothesis is that the aero tail will produce turning speeds and lateral accelerations (measured via an IMU) similar to the inertial tail. The experimental trials were carried out on a football turf field whilst utilizing a drone to capture and analyze the video trials. The tail speed and turning speed were tested for the three test groups namely no tail, inertial tail and aerodynamic tail. Although initial results looked promising, with the aero tail performing better than the inertial tail in terms of turning speed, no conclusions to our hypothesis could be drawn. This was due to motor failure which prevented us from collecting additional data. But statistical analysis shows that with an additional 98 trials per test case we can establish conclusive results.

Introduction

Nature is a fantastic source of inspiration for engineers developing new technological tools. Biomechanics literature defines *maneuverability* as an animal's ability to change its velocity vector in a controlled manner [1][2][3]. This consists of either changing the body's velocity magnitude or adjusting its direction (turning). Tails are used by animals for a variety of purposes, including balancing, swimming, sprinting, climbing, hopping, and flying control. We think that rather than depending on complicated control system algorithms, mobile robots can improve their agility by employing a tail.

Our motivation for this project stems from a video of a cheetah during a pursuit, in which its tail can be seen swinging swiftly from side to side during sharp bends [13]. During quick sprints, the paws of a cheetah make minimal contact with the ground. The cheetah's long muscular tail acts as a rudder, stabilizing and counterbalancing the animal's body weight. Swinging the tail back and forth while constantly reacting to the velocity of the prey allows for quick twists during high-speed chases [4]. Patel *et al*. investigated the aerodynamics of a cheetah tail and discovered some fascinating results. A wind tunnel was used to study the midsection and tip of the tail. They did a simulation of a stiff tail using data from wind tunnel measurements to evaluate the influence of aerodynamic forces on the body. According

to their findings, the cheetah tail may be employed as a 'rudder' to aid in quick heading and as a stabilizer during rapid acceleration and turning [10].

Patel *et al*. studied the cheetah's conical motion using a simplified two-degree of freedom actuated tail. The resulting paper investigates the optimization of tail motions for bioinspired robots. The tailed robot's experiment results showed that it was able to achieve approximately 70% more lateral acceleration than the robot with no tail[5]. Patel *et al.* examined the usage of an actuated tail for a quick turn at high speed in this research. For both tailed and no tail models, the robotic system outperformed the expected velocity. Their findings demonstrate how the tail might improve the stability of running quadruped robots subjected to external shocks [8]. Joseph *et al.* investigated upon the effects of a lightweight aerodynamic tail that swung back and forth for a quadrupedal cheetah robot and found that the aerodynamic drag force provided continuous torque even at zero acceleration[15]. Building upon this, Kohet *et al.* tested the effectiveness of aerodynamic steering on a quadruped robot but with the tail swinging laterally along the body axis and concluded that aerodynamic torque provided stability during steering[17].

Present literature exists, extensively focussing upon the effects of rigid tail dynamics on the maneuverability of a cheetah robot [1,7], and the effects of an aerodynamic sail on legged robots. However the effects of an aerodynamic sail on wheeled robot stability have not explicitly been investigated. Although other works have rotated their aerodynamic tails about the body axis during turning maneuvers, there isn't any literature existing that rotates the sail perpendicular to the axis of the robot body during high speed wheeled robot turning.

Our project aims to analyze the effects of an aerodynamic tail to provide stability for a wheeled robot executing high speed turns and we concluded that an aerodynamic sail is effective to prevent toppling of the robot during this maneuver. We thought that Aerodynamic drag forces from the tail swinging perpendicular to the body axis provide counter torque to the wheeled robot whilst steering through turns and keep it stable. The biological inspiration we are trying to model is shown in Figure 1.

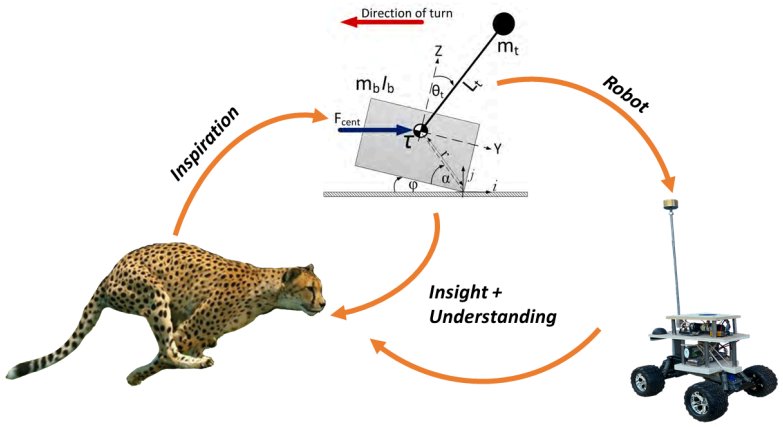

Figure 1: Biological Inspiration for Robot System modeling

Research Question

With the above ideas in mind, the main gap that we aim to fill is to test the effectiveness of an aerodynamic tail on the agility of the robot body and prove that it is a lightweight substitute for the inertial tail. Furthermore, we also plan to test high speed maneuverability by measuring the turning speed for the vehicle executing rapid turns when coupled with an aerodynamic tail. The aim of this test would be to prove that the aerodynamic tail provides stability and agility to the robot when performing this motion just like a cheetah tail provides beneficial effects to a cheetah. We plan to simulate these properties first for the rigid tail and aerodynamic tail design before employing them onto the robot. **We hypothesize that a lightweight aerodynamic tail can be utilized to increase the maneuverability of a wheeled mobile vehicle compared to an inertial tail.**

Design

To achieve the goals for this project, the design process is divided into 3 segments: mobile robot, the inertial tail, and the aerodynamic tail.

Mobile robot

As our research question seeks to extend the speed at which a robot can turn without toppling, we must design the mobile robot to be fast enough to topple itself when turning, thereby giving a baseline target for the tails to improve upon. To make that possible, the center of gravity of a mobile robot should be at a considerable height from the ground. Since this project is focused more on the tail dynamics, rather than designing the mobile robot from the ground up, we bought the same off-the-shelf RC car that Patel *et. al*. [7] used and modified it according to the tail integration requirements. An image of the RC car can be viewed in Appendix C.

We needed to make modifications to the mobile robot that fulfilled our design requirements like supporting the tail assembly that contains the actuator, motor controller, battery and a microcontroller. Therefore, we designed and analyzed a platform assembly to make sure that it could take the load of the tail assembly. For material selection of the platform assembly, we used 3/4” plywood at the chassis and 1/2” plywood as the platform since it was readily available and easy to work with.

During our initial testing, we realized that to withstand the overall load of our tail assembly and the platform, we needed to change the suspension springs of the robot and add metal springs with higher stiffness. We also realized we had to add another layer of ½” mdf wood on top of our electronics to keep them safe during the experiments. Figure 2 illustrates the final prototype of our mobile robot design.

Figure 2: Final design of the mobile robot

Inertial Tail

The preliminary design of the rigid tail is similar to what Patel *et. al.* [7] constructed. Both designs utilize an aluminum rod with a brass weight attached to the end of the tail but we made certain modifications to match our needs. The rod used for the tail in our design was 0.5m long and threaded throughout while Patel's was a solid rod with threading at the end. The brass weight, weighing 0.4 kg, was threaded to allow it to attach to the rod. We could not find a suitable coupler that would allow us to couple the rod and the motor which led us to fabricating our own. We designed the coupler in CAD to have a set screw attachment to the rotor-facing shaft and a threaded attachment to the tail (where the tail rod was selected to be a threaded rod). We selected 6061 Aluminum as the material and verified its robustness to high stress by applying expected virtual loads in a SolidWorks stress analysis study. This analysis confirmed the part would not come close to yielding and can be viewed in Appendix D We then created a dimensioned drawing and fabricated the part within its allowable tolerances (also viewable in Appendix D).

An additional difference between Patel's design and ours was the motor used in the robot. Patel's motor configuration would have cost the team approximately $900, which was not feasible given the $1000 budget. Given this limitation, we performed analysis to determine what output torque our motor would need to provide in order to move the given mass π rad in one second. These calculations can be found in Appendix E and show us that we needed a motor that could provide a torque of approximately 3.2 Nm. Using this baseline torque our team was able to spec out an appropriate motor for our project.

Aerodynamic Tail

In the initial stage of the aerodynamic tail design two crucial questions needed to be answered. The first was the sizing of the tail and the second was the kind of material to be used for the tail design. Ultimately the tail component needed to replicate the features of a sail in that it needed to provide aerodynamic drag in the reverse direction of rotation of the tail so that it can stabilize the vehicle body during turning. The design of the aerodynamic tail was divided into two components, the support, and the sail. The support was of a rectangular shape, having an interior slot to house the sail structure. We conducted extensive analysis by reading through previous literature regarding the sail dimensions and kept it consistent with

existing literature parameters. For the support, we decided to use wood as the material and for the sail, we determined that using PETG would be a good idea. We then conducted simulations of the aero-tail in Ansys Fluent to see the variation in the drag coefficient and drag force with changing sail angles and wind velocity.

We conducted the simulations separately for the sail and the support to see how the two different structures of different materials account for drag production separately. In the simulations, we varied the wind velocity from 0 m/s to 3 m/s and simulated the drag coefficient for a specific sail angle. Then the simulations were run multiple times for sail angles between 0 - 75 degrees. The drag coefficient and drag force graphs are viewable in Appendix F. This process was done twice, once for the sail and once for the support. As expected, the drag coefficient increased with increasing wind speeds. From the separate analysis of the sail and the support, the sail accounted for much more drag than the support. This is most likely because of the difference in the dimensional area between the two entities. The simulations were important as they helped us understand the points of the sail that produced the maximum drag force that would stabilize the robot the best during a high-speed subsonic angular maneuver.

We tried to expand our simulation test cases by increasing the area of the aerodynamic tail and analyzing its effect. This provided better results by yielding a higher drag value. From this, we determined the sail dimensions would be set at 100mm x 200 mm. The optimized results with their drag coefficient and drag force have been appended to Appendix G. After this, we worked on the tail fabrication. We used the Rabbit Laser in Techspark to create our support using 1/4’’ wood. The support housed a sail made of PETG is stuck between two support cutouts using epoxy. The bottom end of the tail had holes drilled in it so that it could be integrated into a 3D print part that houses brass support, which connects to the tail. The 3D printing was also done in Techspark and had holes drilled in it so that it could be fastened onto the aero tail support by means of screws.

(a) (b)

Figure 3: (a) Inertial Tail with coupler (b) Aerodynamic Tail with coupler

Tail Control

As the inertial tail and aerodynamic tail are actuated through the same motor and undergo the same sweeping motion, the controller architecture is the same for both tail systems. Following the standard feedback control diagram, we are using a position reference signal in conjunction with a PID controller to achieve the sweeping motion. We use encoder data from the DC motor at the base of the tail to determine the current position of the motor (in radians). This current position is then subtracted from the target position (the reference signal) and provided as an input to the PID controller.

For our initial tuning and testing, we had built a benchtop setup for the control system consisting of the DC motor, an encoder, a RoboClaw motor controller, a DC power supply, and a laptop loaded with Basic Micro Motion Studio as shown in the Figure 4.a. Basicmicro Motion Studio provided us with a PID tuner and live, simple to use control over the reference signal to the motor. Using this setup, we successfully completed proof of concept tests for the tail subsystem. Furthermore, we wanted to control the tail subsystem based on a microcontroller. To do so, we used an Arduino board which communicates with the motor controller. We also wanted to use an inertial measurement unit (IMU) that tracks the rolling angle of our mobile robot and use that as a reference signal for actuating our tail. To achieve that, we integrated an IMU to the Arduino script and are receiving the rolling data from the IMU to generate these reference signals. The tail is only actuated when rolling angle crosses a certain threshold. This threshold was determined by the angle at which our robot is about to topple over. Figure 4.b shows the block diagram of our circuit. Our PID control diagram and the circuit diagram can be viewed in Appendix H and Appendix I, respectively.

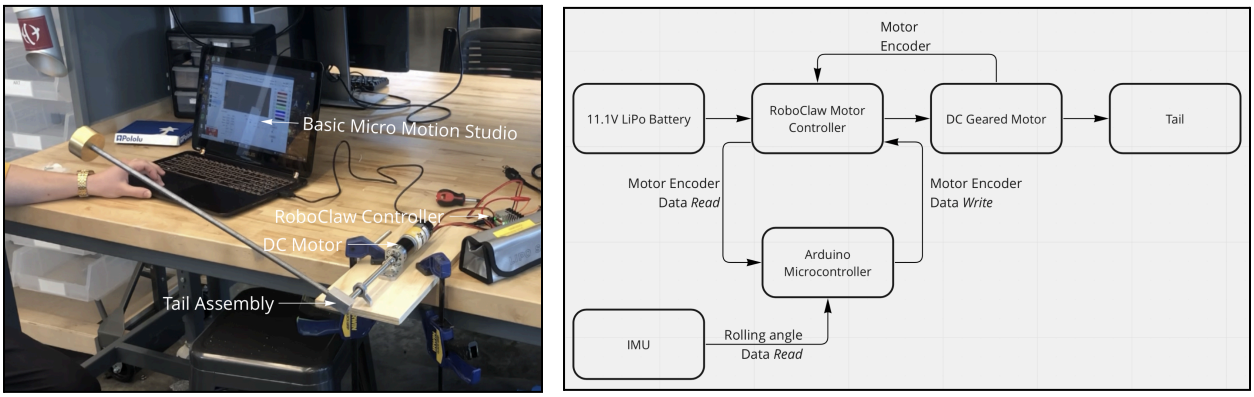

Figure 4: 4.a (left) benchtop setup. 4.b (right) Block diagram of our circuit

Methods

To determine the ability of the aerodynamic tail to increase the maneuverability of the mobile robot, we first need to define how to quantify maneuverability. We chose to characterize maneuverability as a combination of large entry speed and small turning radius in execution of a turn. The three test groups used for experimentation are: the robot without a tail, the robot with the inertial tail attached, and the robot with the aerodynamic tail attached. The robot without a tail in this context acts as the control group or benchmark test group to compare against.

We followed the same procedure for each test group:

1. Drive the robot forward until constant velocity is reached

2. Actuate the steering servo to make a turn (~4° steering angle) for approximately 0.5 seconds, then return to zero steering angle

Note that for the test groups which include a tail, the tail will actuate when the turn causes the roll angle of the robot to exceed the predefined threshold.

To reduce variability, we had the same driver (Pranav) repeat experimental trials. The turf football field was used for each trial and all trials were run on the same day. We did not directly measure the wind velocity but the weather report gave speeds of 5-10 mph on average for the day.

We used a drone to capture overhead video of the trials. A high contrast dot was attached to the top of the robot to make motion tracking easy. These videos were then analyzed in Tracker to determine the entry speed and turning radius of the robot in execution of the turns. Figure 5 shows a snapshot of the Tracker analysis.

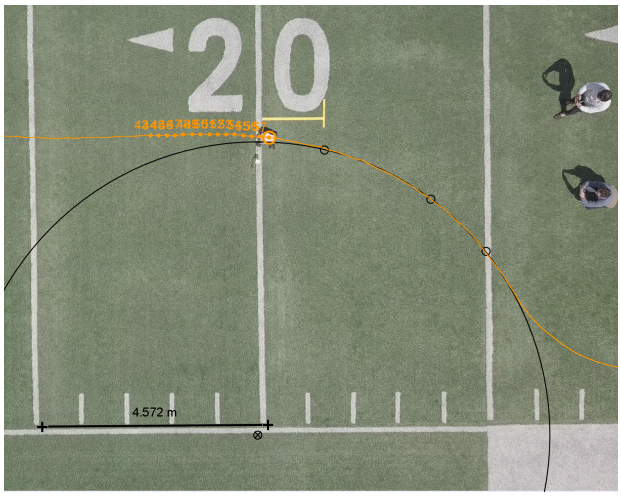

Figure 5: Tracker motion tracking analysis snapshot

We collected a total of six experimental trials before the robot was totalled. The tail motor blew apart during an unsuccessful trial in which the robot failed to turn without rolling over. Because the sample size is so small, we did not perform any statistical techniques on the raw data.

If we were able to record as many trials as we could, we would have performed one-dimensional binomial logistic regression or support vector regression on the data for each test group to determine the decision boundary that defines when the test group succeeds or fails. The independent variable is the entry speed and the dependent variable is a binary pass/fail variable. We would also need to make some assumptions that the turn radius is fixed between trials and a 10% margin of error is captured by all other uncontrollable variables. Quantifying the margin of error is necessary to determine the necessary number of trials.

We would have needed to carry out 98 experimental trials for each test group to have a 95% confidence level in the decision boundary. This analysis shown in Appendix J explains how we arrived at this number of desired samples.

Results

All data used to create the results have been placed in a Google Drive folder and linked at the beginning of our Appendices.

Tail Speed

To verify that the selected tail motor was capable of accelerating and decelerating the tail such that sweep (π rad) was completed within 1 second, we conducted stationary tail swing tests for both the inertial tail and aerodynamic tail. The results are displayed in Table 1 below and indicate that the tail motor is more than sufficient for completing a 1 second swing for either tail. One interesting note is that despite the mass difference between the two tails, the speed profiles associated with each tail are extremely similar. This is likely due to our over speccing of motor stall torque, making the tail mass essentially negligible from a motor speed perspective.

Table 1: Tail Swing Analysis Results: One swing is defined as a sweep of π rad. Peak acceleration and velocity occurred slightly after the apex for both tails. These trails were run while AeroDIMA was stationary. Data was obtained via Tracker.

	Inertial	Aerodynamic
Peak Acceleration	30.90 m/s^2	29.29 m/s^2
Peak Velocity	4.153 m/s	4.009 m/s
Swing Duration	0.633 s	0.667 s

Turning Speed

As described in Methods, maximum turning speed was tested by driving the vehicle linearly at a high speed, then engaging the vehicle in a turn. If the vehicle remains upright throughout the movement, the test is deemed successful and the maximum turning speed is measured as the speed at which the turn is initiated. The results are displayed in Table 2 below indicating that the aerodynamic tail does in fact outperform the inertial tail on the AeroDIMA. Because identifying an exact maximum turning speed is infeasible given the experimental setup, the results should be considered as bounds for a maximum speed. The successful entry speed provides a lower bound of maximum turning speed while the failed entry speed provides an upper bound. Figure 6 helps to visualize these bounds.

Table 2: Maximum Turning Speed Results: Maximum turning speed is defined as the speed at which the vehicle enters a turn. A successful trial occurs when the vehicle maintains an upright position avoiding rollover throughout the duration of the turn. All other outcomes are failed trials. The fastest successful trail and slowest failed trails were used for each tail option to provide the tightest bound on turning speed.

	Success		Fail	
	Entry Speed	Turning Radius	Entry Speed	Turning Radius
No Tail	6.35 m/s	6.5 m	5.70 m/s	6.6 m
Inertial Tail	4.72 m/s	4.3 m	5.77 m/s	5.8 m
Aerodynamic Tail	5.32 m/s	5.9 m	5.86 m/s	4.4 m

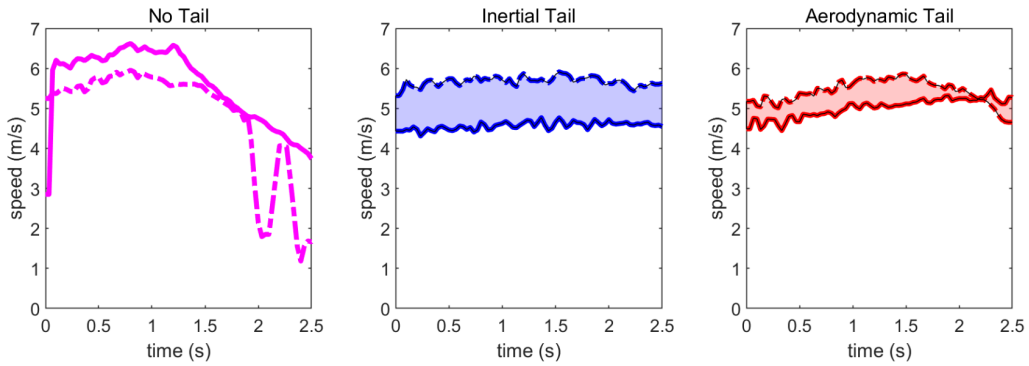

Figure 6: Maximum Turning Speed Bounds: The area between the curves represents the possible region of maximum turning speed. The dotted line corresponds to the failed trail and the solid line corresponds to the successful trial. Note that because the No Tail case has no region under fail but over success, so no area could be filled.

The Maximum Turning Speed Results, shown in Table 2, suggest that AeroDIMA performs best with no tail. While this is an interesting result, it should not be taken blindly as a conclusion. We believe this datapoint is an anomaly and would be ruled as an outlier if more trials were conducted. One hint that this could be the case is that the robot actually failed a wider turning radius at a lower speed (as shown in Table 2).

As mentioned above, we were unable to collect a sufficient number of trials to conduct statistical analysis of the results, which could have proven very useful for substantiating the results. This was not possible due to mechanical failure of the tail motor during testing. The DC motor, gearbox, and faceplate all detached during an inertial tail trial and could not be reassembled.

Conclusion and Future Work

Our initial results suggest that the aerodynamic tail outperforms the inertial tail in terms of maneuverability as it has a higher turning speed than its inertial counterpart. However, our findings are not consistent with those of Patel et.al with regard to the comparison between the no-tail and inertial tail cases. This is due to the fact that our dataset is not large enough to make substantial conclusions. As discussed in the Methods section we would need 98 of additional data points per test case to be able to validate our hypothesis.

Future work would involve enlarging the dataset to help establish an answer to our initial hypothesis. We would also like to remove the factor of human bias by adding a controller to run the RC car. Furthermore, we suggest adding the ability to log the IMU sensor data as another point of reference as well as using a more robust motor for the tail to reduce the likelihood of motor failure when turning. Patel et. al. used a Maxxon configuration with a higher RPM and more robust build.

Although no conclusions could be drawn, our initial testing looks promising. If further work was conducted we are confident that the results would provide a great insight into the effect that aerodynamic drag can have on the locomotion of a tailed robot.

References

[1] A. Patel and M. Braae, "Rapid acceleration and braking: Inspirations from the cheetah's tail," *2014 IEEE International Conference on Robotics and Automation (ICRA)*, 2014, pp. 793-799, doi: 10.1109/ICRA.2014.6906945.

[2] P. W. Webb, “Maneuverability - General Issues,” *IEEE Journal of Oceanic Engineering*, vol. 29, no. 3, pp. 547-555, 2004.

[3] D. Jindrich and M. Qiao, “Maneuvers during legged locomotion,” Chaos, vol.19, 2009.

[4] “About Cheetahs,” *Cheetah Conservation Fund*, 29-Jul-2021. [Online]. Available: https://cheetah.org/learn/about-cheetahs/.

[5] A. Patel and E. Boje, “On the conical motion of a two-degree-of-freedom tail inspired by the cheetah,” *IEEE Transactions on Robotics*, vol. 31, no. 6, pp. 1555–1560, 2015.

[6] R. Briggs, J. Lee, M. Haberland and S. Kim, "Tails in biomimetic design: Analysis, simulation, and experiment," *2012 IEEE/RSJ International Conference on Intelligent Robots and Systems*, 2012, pp. 1473-1480, doi: 10.1109/IROS.2012.6386240.

[7] A. Patel and M. Braae, "Rapid turning at high-speed: Inspirations from the cheetah's tail," *2013 IEEE/RSJ International Conference on Intelligent Robots and Systems*, 2013, pp. 5506-5511, DOI: 10.1109/IROS.2013.6697154.

[8] O. V. Borisova, I. I. Borisov, and S. A. Kolyubin, "Analysis and Modeling of Galloping Robot With Actuated Tail for Balance*," *2020 International Conference Nonlinearity, Information and Robotics (NIR)*, 2020, pp. 1-6, DOI: 10.1109/NIR50484.2020.9290192.

[9] W. Saab, J. Yang and P. Ben-Tzvi, "Modeling and Control of an Articulated Tail for Maneuvering a Reduced Degree of Freedom Legged Robot," *2018 IEEE/RSJ International Conference on Intelligent Robots and Systems (IROS)*, 2018, pp. 2695-2700, doi: 10.1109/IROS.2018.8593945..

[10] Amir Patel, Edward Boje, Callen Fisher, Leeann Louis, Emily Lane; Quasi-steady state aerodynamics of the cheetah tail. *Biol Open* 15 August 2016; 5 (8): 1072–1076. doi: https://doi.org/10.1242/bio.018457

[11] Patel, Amir,2014,“Understanding the Motions of the Cheetah Tail Using Robotics”, PhD Thesis, University of Cape Town, Cape Town

[12] B. Simon, R. Sato, J. Choley and A. Ming, "Development of a Bio-inspired Flexible Tail Systemxs," *2018 12th France-Japan and 10th Europe-Asia Congress on Mechatronics*, 2018, pp. 230-235, doi: 10.1109/MECATRONICS.2018.8495667.

[13] Lion Mountain TV, “Cheetah High Speed Gazelle hunt | classic wildlife,” *YouTube*. [Online]. Available: https://www.youtube.com/watch?v=EcgJPDxwKNI.

[14] Stampede®: 1/10 scale monster truck with TQ™ 2.4GHz Radio System
https://traxxas.com/products/models/electric/base-stampede-36054-4?t=spec

[15] Aerodynamic Steering of a 10 cm High-Speed Running Robot N.J. Kohut, D. Zarrouk, K. C. Peterson and R. S. Fearing

Appendices

Data Used for Results:
https://drive.google.com/drive/folders/1IPel1kX_8Olpwhk0zKhR1ZwYd1Vw_dkC?usp=sharing

Appendix A: Individual Technical Contribution

Role	**Explanation of Each Role**	**Person in charge or develop this expertise**
Car: Design Modification	Focuses on designing a platform to place all the electronics and supporting structure on the RC car	Harshal, Ryan
Aerial Tail: Design	Creating multiple aerodynamic shapes of the tail and creating a CAD	Aishwarya
Aerial Tail: Analysis	Analyzing the multiple aerodynamic tails to identify which is suited for our project	Saurabh
Aerial Tail: Optimization	Optimizing the shape of the tail to make it more aerodynamic	Aishwarya
Inertial Tail: Design & Analysis	CAD model of the rigid tail and analysis to characterize potential failure modes	Pranav
Overall Tail: Motor Selection	Analysis to determine the required motor torque to move the tail in the required direction within a set amount of time	Pranav, Zach
Overall Tail: Controls	Controlling the both the tails given different conditions	Harshal
System: Modeling & Analysis	Modeling and analyzing the whole system to verify the design parameters	Zach
System: Integration	Integrating the vehicle and tail system to work as one	Ryan, Saurabh
System: Fabrication	Manufacturing	Ryan

Harshal: I was responsible for designing and analyzing the platform on which all the electronics and tail assemblies were mounted. I was also responsible for 3D printing the necessary components for the platform assembly with the RC car. I also helped on controlling the tail actuation using an IMU, an Arduino and the motor controller. Lastly, I was the project manager for this project and I was responsible for planning and developing the project plan, and making sure we achieved all the milestones we set for the project.

Pranav: Responsible for designing and analyzing the inertial tail setup. With Zach's help, this analysis was then used to select the motor we used. I also took responsibility for the technical writing aspects by

editing and correcting documentation that our team submitted. I worked on the IMU setup and initialization. I was also responsible for placing and picking up orders as well as budgeting, the latter of which Harshal and Zach assisted with. I lent a helping hand wherever needed like assisting with laser cutting for the aero tail and 3D printing of the chassis.

Saurabh Patil: I was responsible for running the simulations on the sail at varying angles and wind velocities. Through simulations, we found out the drag coefficients and drag force. I also worked on optimizing the shape of the sail, so that the aerodynamic tail produces higher drag force and better maneuverability as compared to the inertial tail. I was also responsible for 3D printing the support that connects the sail part of the aero tail and the rod. I also contributed to the tail control via the Arduino and implementing the IMU as well.

Ryan: I designed and created the GD&T drawing of the right-angle coupler used to couple the drive shaft to the tail. I carried out stress analysis in SolidWorks to ensure the part would not yield or fracture when experiencing the expected torques and loads given its geometry and a material type (Al 6061). The figure in Appendix E shows the part loaded with 10x higher than anticipated torques and loads. I also helped with the platform design and completed most of the fabrication along with Zach. I also performed the statistical analysis needed to determine how many more data points we need to establish conclusive results.

Zach: I helped spec and select a motor for the tail with Pranav. Pranav, Ryan, and I also designed the tail transmission system (brackets, shafts, couplings). I selected the electronic components needed to power the tail motor (motor controller and battery). I helped get the motor controller working with our tail motor. I helped fabricate the chassis support and platform with Ryan (and others). I conducted the motion tracking analysis using Tracker. I accidentally bought really big zip ties because the pictures online didn't look that big.

Aishwarya: I created the CAD drawings of the aero tail and performed the simulations on the support of the aerodynamic tail for varying wind velocities and varying sail angles to obtain the drag force and drag coefficients. I worked on the material analysis of the sail and support to see the variation of drag forces for various materials used. I also calculated the counter drag forces that were needed to overcome the tail and analyzed the flow streamlines for the structure. I helped in the manufacturing of the support by laser cutting wood that holds the sail.

Appendix B: Budget

Supplier	Item	Quantity	Price	Total Price + Taxes
Traxxas	Mobile Robot	1	$211.00	$223.66
ServoCity	DC Geared Motor	1	$39.99	$51.38
ServoCity	M4 x 0.7mm x 16mm screw	1	$3.79	$4.02
ServoCity	Right-Angle Mounting Bracket	1	$8.49	$9.00
Pololu	RoboClaw 2x15A Motor Controller	1	$124.95	$138.90
McMaster Carr	Spring	1	$5.71	$6.05
McMaster Carr	M5 x 0.8mm x 16mm screw	1	$5.61	$5.95
McMaster Carr	M5 Nut	1	$5.63	$5.97
Amazon	11.1V LiPo Battery	1	$29.99	$31.79
Amazon	IMU	1	$9.99	$10.59

Amazon	LiPo Charger	1	$12.99	$13.77
Amazon	LiPo Safe Bag	1	$7.99	$8.47
ServoCity	Pillow Block (3/8" Bore)	2	$6.99	$14.82
ServoCity	0.375" to 6mm Shaft Coupling	1	$4.99	$14.28
McMaster Carr	3/8" x 6" SS shaft (Part no: 89535K87)	1	$22.45	$23.80
McMaster Carr	Back Springs	1	$8.83	$9.36
McMaster Carr	Machinable Brass Weight	1	$37.46	$37.46
McMaster Carr	Threaded Rod (3/8" x 2')	1	$10.54	$10.54
McMaster Carr	Brass Insert (3/8" x 0.5")	1	$10.79	$10.79
N/A	3D Print Filament	1	$10.00	$10.00
Techspark 3D print	3d print aero tail support	1	$21.00	$21.00
Techspark 3D print	3d print aero tail support	1	$2.50	$2.50
Techspark 3D print	3d print aero tail support	1	$2.50	$2.50
Techspark	¼” wood	1	$4.00	$4.00
McMaster Carr	Right Angle Bracket	10	$0.90	$9.00
McMaster Carr	8" Velcro w/ Buckle	3	$1.55	$4.65
McMaster Carr	10-32 1.5" Bolts (50pk)	1	$14.88	$14.88
McMaster Carr	4" Hex Standoffs w/ 10-32 thread	10	$11.92	$119.20
McMaster Carr	Adhesive Bumper	2	$8.49	$16.98
McMaster Carr	Nylon Zip Ties (24", 10pk)	1	$4.40	$4.40
McMaster Carr	Velcro Strip 5ft	1	$5.38	$5.38
McMaster Carr	Baseboard-Mount Door Stop	4	$1.65	$6.60
			Total Amount	$851.67

Appendix C: Traxxas Stampede car [14]

Appendix D: Coupler Drawing and FEA

Coupler was made of 6061 Aluminum. All dimensions in the drawing are in inches

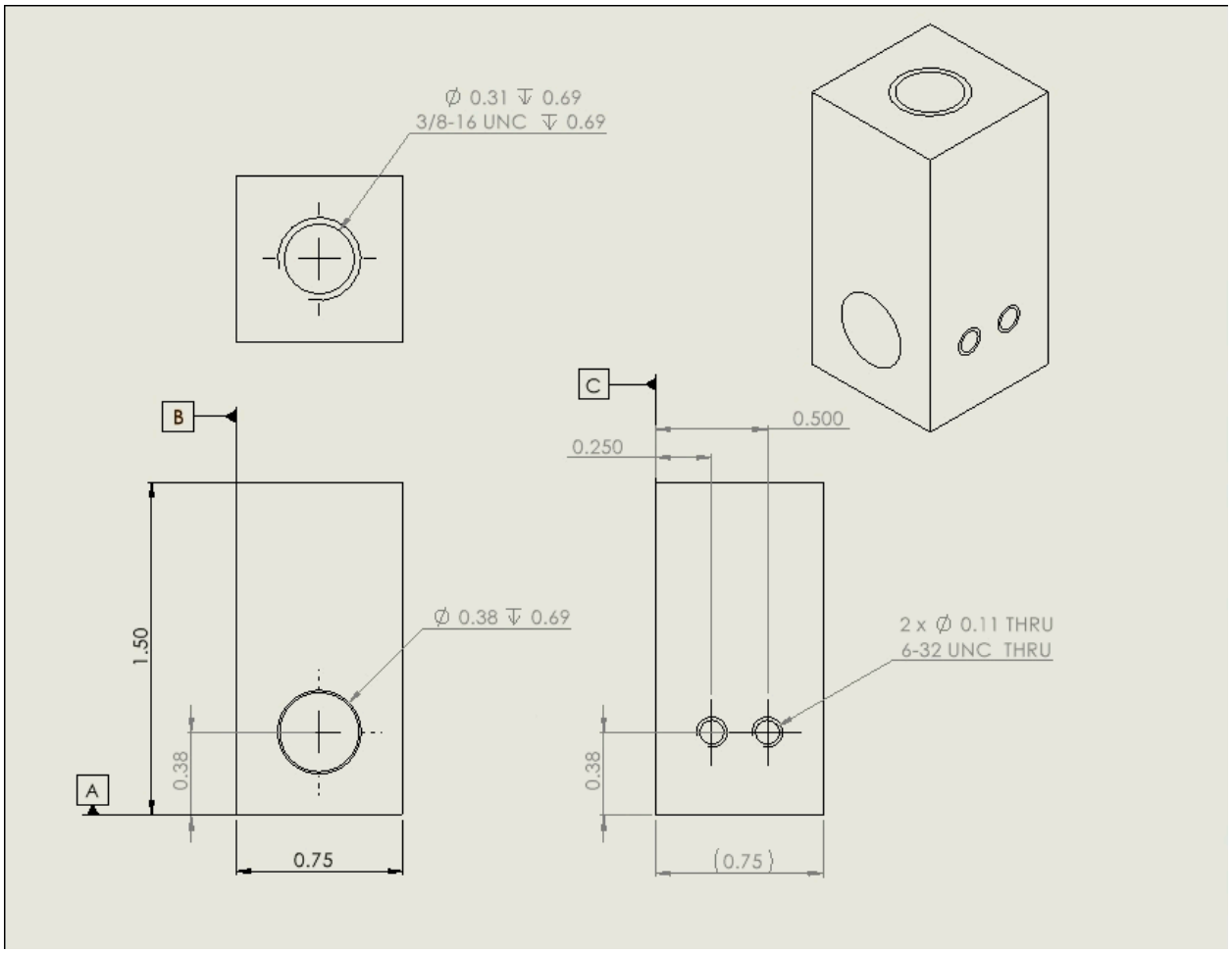

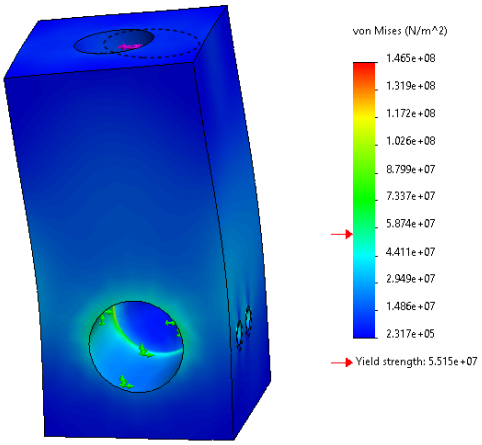

Appendix E: Inertial Tail Calculations

Torque Required:

Assumptions:

- No friction
- Constant accleration
- Point mass

System Parameters:

$m_{\text{rod}} = 0.1\ \text{kg} \quad m_w = 0.4\ \text{kg}$

$\ell_r = 0.5\ \text{m} \quad \ell_m = 0.1\ \text{m}$

$\theta_i = 0\ \text{rad} \quad \theta_f = \pi\ \text{rad}$

$t_f = 1\ \text{sec}$

Procedure:

$$\omega = \frac{\Delta\theta}{\Delta t} = \pi\ \frac{\text{rad}}{s}$$

$$\alpha = \frac{\Delta\omega}{\Delta t} = \pi\ \frac{\text{rad}}{s^2}$$

$$a = r\alpha = 0.55(\pi) = 1.728\ \frac{m}{s^2}$$

$$F = (m_r + m_w)a + (m_r + m_w)g = 5.769\ \text{N}$$

$$T = F\left(\ell_r + \frac{\ell_m}{2}\right) = 3.17\ \text{Nm}$$

Appendix F: Drag Coefficient and Drag Force Graphs

- **CFD Model used**:- Standard k-epsilon model with default parameters
- **Boundary Conditions**:- Inlet:- Varying velocity values ranging from 0 to 3 m/s
  Outlet:- Pressure

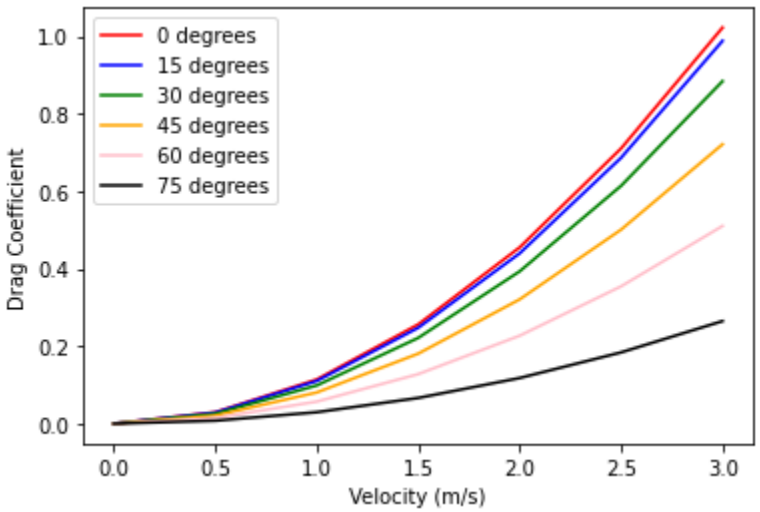

Drag coefficient vs Wind Velocity at different sail angles

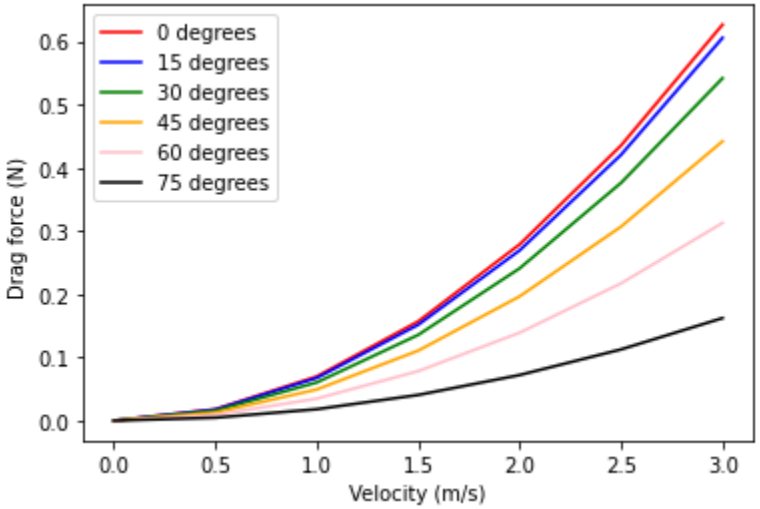

Drag force vs Wind Velocity at different sail angles

Appendix G: Sail Dimensions

Table 3: Optimization of sail dimensions to increase drag coefficient and force

Dimension (width x height) (mm)	Velocity (m/s)	Drag Force (N)	Drag Coefficient
100 x 200 (optimized)	0	0	0
	0.5	0.043194	0.070521
	1	0.169388	0.276551
	1.5	0.381149	0.622285
	2	0.677701	1.10645
	2.5	1.059244	1.729378
	3	1.525489	2.490594
80 x 150 (original)	0	0	0
	0.5	0.017965	0.029331
	1	0.069882	0.114093
	1.5	0.156954	0.256251
	2	0.278739	0.455084
	2.5	0.435229	0.710579
	3	0.626399	1.022692

Appendix H: PID control diagram

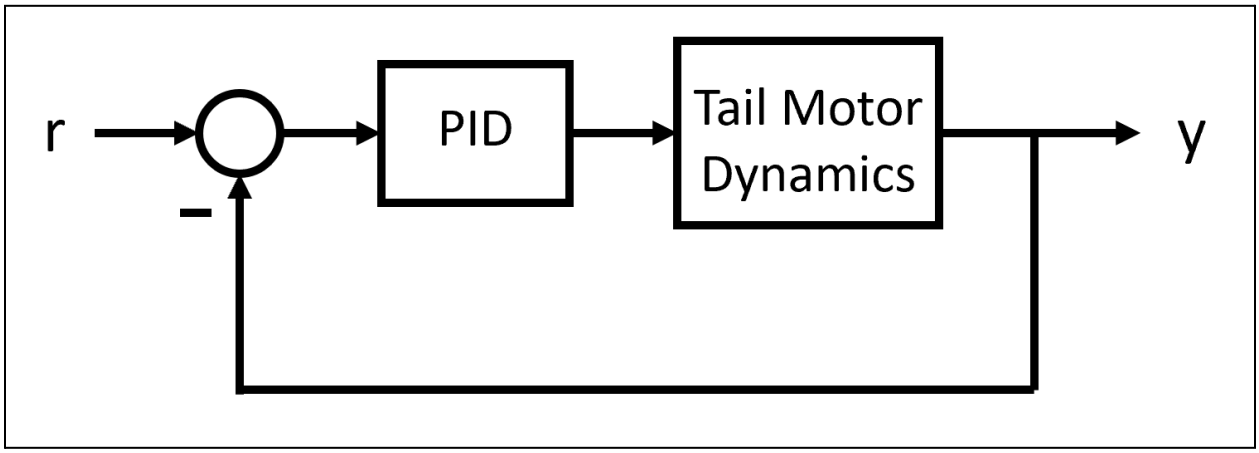

Appendix I: Circuit diagram of our electronics with pin numbers

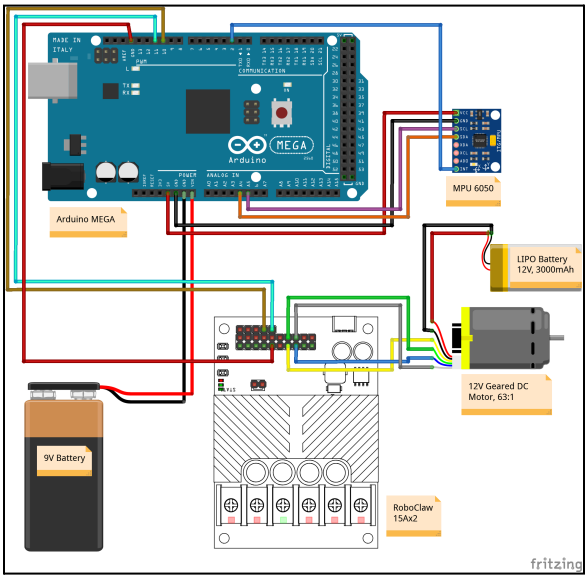

Wire Connections			
MPU-6050	**Arduino**	**RoboClaw**	**DC Motor**
		ENC 1 (+)	Ch. A
		ENC 2 (-)	Ch. B
		+	VCC
		-	GND
	11	S1	
	10	S2	
	GND	S1 (-)	
VCC	5V		
GND	GND		
SCL	A5		
SDA	A4		
INT	2		

Appendix J: Determining desired number of experimental trials

To determine the number of trials for a test group, we first need the desired confidence level and the margin of error. We select the most commonly used 95% confidence level (1.96 z-score) and assume a 10% margin of error. Using the following formula,

$$n = \frac{z^2 \times \hat{p}(1-\hat{p})}{\varepsilon^2}$$

we 97 for the desired number of trials. However, at least two data points (one pass and one fail) are needed to define a decision boundary. Therefore, we actually need 98 total experimental trials per test group to meet our desired confidence level.